JOURNAL OF GUIDANCE, CONTROL, AND DYNAMICS
Vol. 20, No. 2, March–April 1997

Minimax Optimal Control Analysis of Lateral Escape Maneuvers for Microburst Encounters

H. G. Visser*
Delft University of Technology, Delft 2600 GB, The Netherlands

This study examines the optimization of lateral escape trajectories in a microburst wind flowfield for an aircraft on final approach. The performance index being minimized is the maximum value of altitude drop at any point along the trajectory. In contrast to earlier work, the Chebyshev minimax performance index has not been approximated by a Bolza integral performance index. Rather, true Chebyshev solutions have been established by transforming the minimax problem into an equivalent optimal control problem with state variable inequality constraints. In comparison with Bolza solutions, Chebyshev solutions demonstrate a marked improvement in reducing the peak value of altitude drop. Moreover, the general trajectory behavior turns out to be radically different. In Chebyshev solutions, altitude typically is traded for airspeed in the initial phase of the encounter, such as to position the aircraft in a region of relatively low downdraft. The overall benefits of lateral escape vis-à-vis nonturning escape were reconfirmed in this study.

I. Introduction

LOW-LEVEL windshear phenomena, and most notably microbursts, have long been recognized as potential hazards to aircraft in takeoff or approach-to-landing. A microburst is a shaft of cold air that descends rapidly, striking the ground and producing winds that diverge radially from the impact point. Flight crews need to be warned in time to avoid the hazard region or to escape in the event that avoidance is not possible. Most modern jet airliners are currently fitted with a reactive windshear sensor system that permits in situ detection of such potentially hazardous situations. Now in development are forward-look windshear detection systems to look ahead of the aircraft, thus offering improved alert times. Extensive research efforts also have been devoted to the development of escape techniques that can be applied to prevent a possible crash resulting from a microburst encounter. Optimal trajectory studies have contributed significantly to insight about how to best fly an aircraft in a windshear encounter.[1]

The pioneering work in this area is due to Miele et al.[2–4] In addition to optimal control studies to improve the takeoff performance during microburst encounters,[2] they also have considered several approach-to-landing cases.[3,4] Upon encountering a microburst in a glideslope approach, the pilot has essentially two options: to abort the landing or to proceed. If the altitude at which the windshear warning is received is sufficiently high, aborting the approach is the safer procedure. Miele et al.[4] considered optimal abort-landing trajectories through windshears that minimize the peak value of the altitude drop. However, these trajectories were confined to a vertical plane only. Following Miele's lead, the abort-landing results were later extended to flight in three dimensions, i.e., to optimal trajectories that feature lateral maneuvering.[5]

The performance index considered in both Refs. 4 and 5 is of the so-called minimax (or Chebyshev) type. Via suitable transformations,[6] such a Chebyshev problem can be approximated by a Bolza problem. In Ref. 5 it was noted that instead of the Bolza performance index approximation, it is also possible to apply another transformation technique to solve the original minimax problem. More specifically, the minimax problem can be reformulated as a standard optimal control problem with state variable inequality constraints.[7–10] Although the numerical treatment of the resulting Multipoint-boundary value problem (MPBVP) is rather cumbersome, the nonturning escape trajectory results in Refs. 7 and 8 were found to be sufficiently intriguing to warrant a closer examination of this approach. The main purpose of the present paper therefore is to establish optimal lateral escape trajectories by solving the original minimax problem ("Chebyshev solutions") and to compare the results with solutions to the Bolza performance index approximation ("Bolza solutions").

In Ref. 11, Zhao and Bryson propose an alternative formulation for optimization of flight paths in the presence of windshear, namely, maximization of the final value of specific energy while taking into account a safe minimum altitude constraint. It will be shown here that this particular formulation can be conveniently included in the minimax optimal control analysis without significant modification.

Finally, it is noted that the ultimate goal of our research effort is development of a near-optimal feedback lateral-escape strategy for microburst encounters.[12] The present open-loop optimal control results primarily serve to set "ideal" standards against which simulated closed-loop guidance solutions can be compared.

II. Microburst Encounter Modeling

To formulate the equations of motion, a moving but nonrotating reference frame translating with the local air mass is used (relative wind-axes reference frame). With the premises outlined in Ref. 5, the equations of motion describing the dynamics of a point-mass modeled vehicle moving in the three-dimensional space can be written as follows:

$$\dot{x} = V\cos\gamma\cos\psi + W_x \tag{1}$$

$$\dot{y} = V\cos\gamma\sin\psi + W_y \tag{2}$$

$$\dot{h} = V\sin\gamma + W_h \tag{3}$$

$$\dot{E} = \frac{\left(\beta T_{\max}\{1-[(\alpha+\delta)^2/2]\} - D\right)V}{W} + W_h - \frac{V}{g}[\dot{W}_x\cos\gamma\cos\psi + \dot{W}_y\cos\gamma\sin\psi + \dot{W}_h\sin\gamma] \tag{4}$$

$$\dot{\gamma} = \frac{g}{V}\left[\frac{L+\beta T_{\max}(\alpha+\delta)}{W}\cos\mu - \cos\gamma\right] + \frac{1}{V}[\dot{W}_x\sin\gamma\cos\psi + \dot{W}_y\sin\gamma\sin\psi - \dot{W}_h\cos\gamma] \tag{5}$$

$$\dot{\psi} = \frac{g}{V\cos\gamma}\frac{L+\beta T_{\max}(\alpha+\delta)}{W}\sin\mu + \frac{1}{V\cos\gamma}[\dot{W}_x\sin\psi - \dot{W}_y\cos\psi] \tag{6}$$

$$\dot{\beta} = (1/\tau)[\beta_t - \beta] \tag{7}$$

Received June 10, 1996; presented as Paper 96-3374 at the AIAA Atmospheric Flight Mechanics Conference, San Diego, CA, July 29–31, 1996; revision received Nov. 22, 1996; accepted for publication Nov. 25, 1996.

*Lecturer, Faculty of Aerospace Engineering. Senior Member AIAA.

where x, y, and h are the position coordinates, E is the specific energy, γ is the flight path angle, ψ is the heading angle, and β is the throttle response. The wind velocity vector has three components: W_x, W_y, and W_h. The thrust is assumed to have a fixed inclination, δ, relative to the zero-lift axis. The throttle response is modeled as a first-order lag with time constant τ.

The three control variables in the system model are all subject to inequalities

$$0 \le \beta_t \le 1 \tag{8}$$

$$|\mu| \le \mu_{\max} \tag{9}$$

$$0 \le \alpha \le \alpha_{\max} \tag{10}$$

where β_t is the throttle setting, μ is the bank angle, and α is the angle of attack.

As in Ref. 5, instantaneous angle of attack and roll angle response have been assumed here. This contrasts with the work of Miele et al.,[2–4] where not only is a bound imposed on the maximum value of the angle of attack but also the rate of change of this variable is limited. The validation effort reported in Ref. 13, where the $\dot{\alpha}$ constraint was included in the system model, revealed that the influence of the $\dot{\alpha}$ constraint remains limited to the initial transient only, leaving the overall trajectory behavior and performance virtually unaffected.

The aerodynamic forces lift (L) and drag (D) are modeled in the usual fashion:

$$L = C_L(\alpha)\tfrac{1}{2}\rho V^2 S, \qquad D = C_D(\alpha)\tfrac{1}{2}\rho V^2 S \tag{11}$$

The maximum available thrust force $T_{\max}$ is assumed to be a function of airspeed only. The aircraft type used in the investigation is a Boeing 727. Details of the aerodynamic and thrust data for this aircraft type (in landing configuration) are given in Ref. 5; a detailed description of the microburst wind fieldflow model can also be found there. For this reason, further details regarding the models are omitted here. However, it is recalled that in view of the axisymmetric character of the microburst model, polar coordinates have been used to describe the wind flowfield in a horizontal plane (see Fig. 1).

For a given aircraft position (x, y), it is readily clear from Fig. 1 that the radial distance r from the microburst center (axis of symmetry) located at the point (x_c, y_c) can be computed from the relation

$$r = \sqrt{(x - x_c)^2 + (y - y_c)^2} \tag{12}$$

Also observe that the origin of the coordinate frame is located at the runway threshold. Using polar coordinates, the horizontal wind components W_x and W_y can be readily related to the radial wind velocity W_r:

$$W_x = \cos\psi_w W_r(r), \qquad W_y = \sin\psi_w W_r(r) \tag{13}$$

where ψ_w is the direction of the radial wind velocity vector.

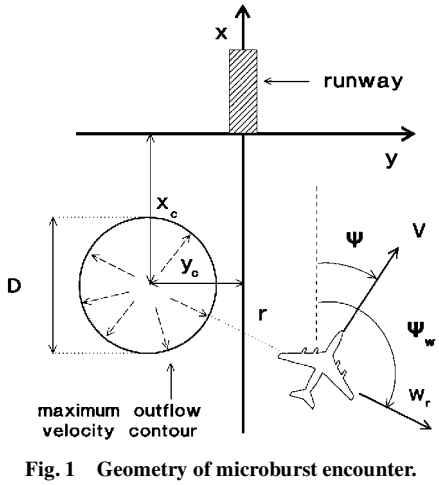

Fig. 1 Geometry of microburst encounter.

An important parameter used in evaluation of windshear performance is the F factor. The F factor can be defined in various ways; here the definition introduced in Ref. 5 for analysis of three-dimensional windshear encounters is used:

$$F \triangleq \frac{(\beta T_{\max} - D)}{W} - \frac{\dot{E}}{V} \tag{14}$$

The F factor represents a direct measure of the degradation of an aircraft's capability to gain energy due to the windshear.[5]

III. Optimal Control Formulation

A. Minimax Optimization Criterion

Because we seek to avert an impending crash, a natural choice for the objective in an abort approach-to-landingis maximization of the terrain clearance, or, in other words, maximization of the minimum altitude at any point along the escape trajectory. An equivalent specification of the performance measure is to minimize the peak value of altitude drop, i.e., the difference between a constant reference altitude h_{ref} and the instantaneous altitude (see Fig. 2):

$$\min I = \min\left\{\max_{0 \le t \le t_f} [h_{\text{ref}} - h(t)]\right\} \tag{15}$$

where $[0, t_f]$ is the fixed flight time interval. Note that the reference altitude h_{ref} needs to be chosen so that the right-hand side of Eq. (15) remains positive at all times.[8] On the basis of a well-known result obtained from functional analysis,[6] i.e.,

$$\lim_{k \to \infty}\left\{\int_0^{t_f} [h_{\text{ref}} - h(t)]^{2k}\, dt\right\}^{1/2k} = \max_{0 \le t \le t_f} [h_{\text{ref}} - h(t)] \tag{16}$$

the minimax criterion in Eq. (15) (Chebyshev performance index) can be approximated by a Bolza performance index

$$\min J = \min \int_0^{t_f} (h_{\text{ref}} - h)^n\, dt \tag{17}$$

where n is a large positive, even exponent. A numerical value for the exponent in Eq. (17) that is typically assumed in many numerical studies[4,5,7,11] is $n = 6$. In normalized form, the Bolza index is denoted here as J_1:

$$J_1 = \int_0^{t_f} \left(1 - \frac{h}{h_{\text{ref}}}\right)^n dt \tag{18}$$

Unless stated otherwise, a power $n = 6$ will be assumed in J_1.

B. Transforming a Minimax Problem into a Standard Optimal Control Problem

Although minimax problems arise in many applications, they are relatively difficult to handle numerically. One of the most commonly used approachesis to apply the transformationtechnique of Warga.[10] By this technique, the minimax problem can be converted into a standard optimal control problem, albeit with the complication of an added state inequality constraint. Let us introduce the maximum altitude drop $\zeta(t)$ as a new state variable:

$$\zeta(t) \triangleq \max_{0 \le \hat{t} \le t_f} [h_{\text{ref}} - h(\hat{t})] \tag{19}$$

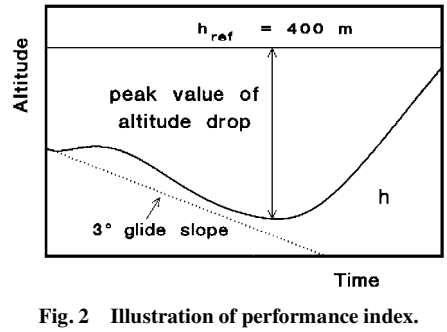

Fig. 2 Illustration of performance index.

The Chebyshev index (15) can now be expressed as an end-cost function J_2:

$$J_2 = \zeta(t_f) \tag{20}$$

subject to the additional constraints

$$\dot{\zeta} = 0 \tag{21}$$

$$S[h(t), \zeta(t)] = h_{\text{ref}} - h(t) - \zeta(t) \leq 0 \tag{22}$$

Effectively, this transformation technique amounts to enforcing a minimum safe altitude constraint (i.e., $h \geq h_{\min}$) while maximizing the minimum altitude limit $h_{\min}(= h_{\text{ref}} - \zeta)$.

C. Final Specific Energy Criterion

The two criteria J_1 and J_2 aim at providing the best possible performance in terms of recovery altitude. However, another important concern is limitation of the energy drain due to windshear, as this directly affects an aircraft's potential to survive in a protracted encounter. To address this issue, a third criterion involving maximization of specific energy at termination is considered:

$$J_3 = -E(t_f) \tag{23}$$

Obviously, the minus sign in Eq. (23) stems from the fact that we seek to minimize the performance index J_3.

D. Composite Performance Index

To permit a tradeoff between the various performance criteria, the following composite index is formed:

$$\begin{aligned}\bar{J} &= \int_0^{t_f} \left(1 - \frac{h}{h_{\text{ref}}}\right)^n \mathrm{d}t + K_1\zeta(t_f) - K_2 E(t_f) \\ &= J_1 + K_1 J_2 + K_2 J_3\end{aligned} \tag{24}$$

where K_1 and K_2 are (positive) weight factors.

To facilitate the numerical computation of the optimal trajectories, a continuation process has been used in which the parameters K_1 and K_2 served as homotopy parameters. Obviously, the homotopy chain was started with $K_1 = K_2 = 0$, which corresponds to the previously established results involving the integral performance measure only.[5] Note that because for any finite value of K_1 there will always be an integral part in the composite performance measure (24), the specification of a "pure" Chebyshev performance measure is precluded.

The main reason for introducing the performance index (24) is that we actually seek to avoid the formulation of a pure Chebyshev optimal control problem. It is well known that many minimax problem formulations are plagued by serious concerns regarding the existence and uniqueness of the solution, particularly when fixed final time problems are considered.[9]

Any attempt to increase specific energy at termination typically comes at the expense of a lower recovery altitude. As a matter of fact, this has been the very reason for including a minimum safe altitude constraint in the maximum final energy analysis of Ref. 11. By employing the composite performance index (24), analysis of Ref. 11 can be completely embedded in the present study. The actually achieved minimum altitude is a function of the weight factor K_2; the larger K_2, the lower the achieved minimum altitude. To reproduce the results of Ref. 11, one needs only to search for the value of K_2 that produces the trajectory for which the actually achieved minimum altitude matches the specified safe minimum altitude.

E. Baseline Scenario

In the numerical examples of Ref. 5, different locations of the microburst have been considered, such as to assess the influence on the escape procedures. However, in this study the main interest is on comparing solutions for different weight factors in the performance index. For this reason, the numerical examples included in this study have been limited to the reference scenario defined in Ref. 5. In other words, only encounters in which the microburst center is located on the runway centerline extension 1.5 km from the runway threshold are considered. The final time t_f has been fixed at 50 s, which is sufficiently large to allow a complete transition of the shear region. For the reference altitude h_{ref}, a value of 400 m has been taken, which, for the assumed flight time, is large enough to ensure that in the trajectory computations h_{ref} will never be exceeded.

The aircraft initial conditions specified in Ref. 5 are also adopted here. These values correspond to a situation in which an aircraft would fly during a stabilized glideslope approach 2.5 km from the runway threshold. It is noted that, for the considered microburst size and location, the aircraft position at which the escape is commenced is on the maximum radial outflow velocity contour. From an operational perspective, the assumed scenario is, therefore, representative of an encounter featuring in situ windshear detection.

Similar to Ref. 5, no terminal boundary conditions on the state variables have been imposed, primarily because such conditions hardly influence the minimum altitude performance but rather affect only the extremal solution in the aftershear region.

F. Necessary Conditions of Optimality

To summarize, the objective is to minimize the composite performance criterion (24) for a given final time, subject to the differential system given by Eqs. (1–7) along with Eq. (21). This system is complemented by the control inequality constraints (8–10) and the state inequality constraint (22). Now that the optimization problem is in a standard form, the basic necessary conditions of optimal control theory for problems involving state/control inequality constraints can be readily applied.

To this end, let us first examine the nature of the state constraint (22). Taking consecutive time derivatives of the equation $S = 0$:

$$\dot{S} = -\dot{h}(t) - \dot{\zeta}(t) = -\dot{h}(t) = 0 \tag{25}$$

$$\begin{aligned}\ddot{S} &= -\ddot{h}(t) = -[V\cos\gamma\,\dot{\gamma} + \dot{V}\sin\gamma + \dot{W}_h] \\ &= -g\left[\sin\gamma\,\frac{T\left[1 - \frac{1}{2}(\alpha+\delta)^2\right] - D}{W}\right. \\ &\quad \left. + \cos\gamma\,\frac{L + T(\alpha+\delta)}{W}\cos\mu - 1\right] = 0\end{aligned} \tag{26}$$

it can be concluded that the state constraint (22) is of second order. Note that in the evaluation of Eqs. (25) and (26), we have used Eqs. (21), (6), and (7), along with the relationship

$$E \triangleq h + (V^2/2g) \;\Rightarrow\; \dot{V} = (g/V)[\dot{E} - \dot{h}] \tag{27}$$

Also note that Eq. (26) explicitly contains the three control variables but that no wind terms are present.

Typical of a second-order state constraint, it can become active in two different fashions, namely, at an isolated point (touch point) or on some subinterval of $[0, t_f]$. Obviously, an optimal path may contain multiple touch points and constrained subarcs. For each specific combination of constrained subarcs and touch points, a different MPBVP results from the application of the necessary conditions. Depending on the factors K_1 and K_2 and the specified aerodynamic roll angle limit $\mu_{\max}$, four different possibilities of active state constraints have been found for the present windshear problem, including the two standard cases, namely, 1) a single touch point and 2) a single constrained subarc. The two other cases are 3) a constrained arc followed by a touch point and 4) two consecutive touch points. However, at this stage we cannot completely rule out the possibility of other combinations. A complete derivation of the MPBVP for each case is presented in Ref. 14.

G. Numerical Implementation

The standard transformation of the minimax optimal control problem into a state-constrained optimal control problem allows numerical treatment of the resulting MPBVP by the multiple-shooting technique. For resolution of the problems formulated, we have employed the well-known BOUNDSCO code that has also been used in previous work.[5,7–9]

Each of the four aforementioned cases of active state constraints requires a specific implementation in BOUNDSCO. Unfortunately, for a given windshear encounter scenario it is not generally possible to tell a priori which is the appropriate case. As a result, some trial and error is typically required.

IV. Numerical Results

A. Assessing the Bolza Criterion

Although the Bolza performance index approximation (18) has been widely used, the accuracy of the resulting solutions has not yet been properly assessed. For this reason, an attempt has been made to compute optimal Bolza solutions for values of the exponent n in the performance index (18) larger than 6. Because of numerical complications in the solution, it is not generally possible to use very large values for n. However, we have been able to compute optimal trajectories with exponents up to 16, albeit with great difficulty.

Note that for the best possible computational results, the reference altitude h_{ref} should be chosen as small as possible with the difference $h_{\text{ref}} - h$ positive at all times. Because the actually achieved maximum altitude within the specified time interval depends on the particular scenario that is considered (e.g., the microburst location), the parameter h_{ref} must be selected carefully so that it can apply in all situations.

The following numerical example serves to illustrate the minimum altitude performance of optimal trajectories computed for a sequence of exponents n in the Bolza performance index (18). Three different values of the exponent n are considered in Fig. 3, namely, $n = 6$, 8, and 10. For reference purposes, the corresponding Chebyshev solution (see next section) has also been included. This particular solution has been labeled $n = \infty$ in Fig. 3. Although not directly apparent from Fig. 3, the trajectories shown concern lateral maneuvers that are executed with an assumed aerodynamic roll angle limit of 10 deg.

From Fig. 3a it is readily observed that the Bolza performance index approximation J_1, featuring $n = 6$, produces rather unsatisfactory results in terms of minimum altitude performance. Increasing the power n from 6 to 8 results in a vast improvement, despite the fact that the angle-of-attack behavior is not significantly affected (see Fig. 3b). Increasing the power n even further, from 8 to 10, raises the minimum altitude to a higher level, and the initial climb disappears. However, a comparison of the Bolza solution with $n = 10$ with the Chebyshev solution clearly shows that the minimum altitude performance is still rather poorly approximated.

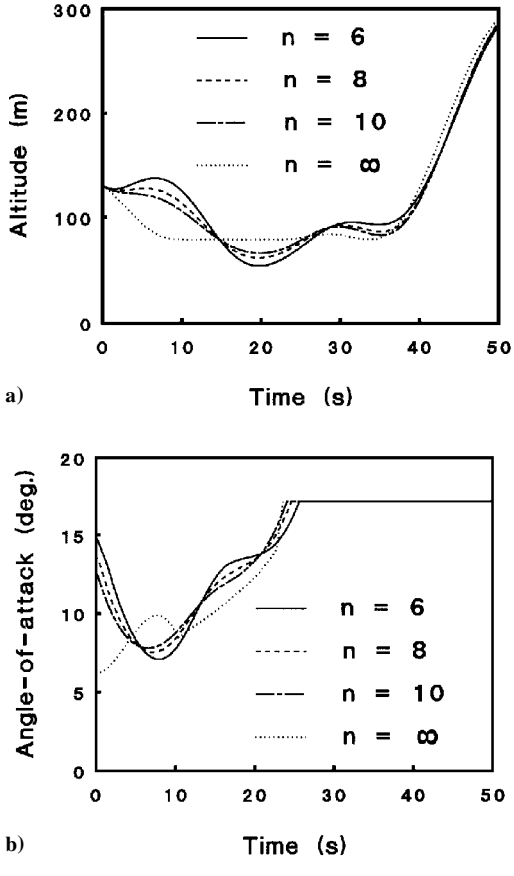

Fig. 3 Comparison of extremal solutions for various values of the exponent n in the performance index J_1; lateral maneuvering ($\mu_{\max}$ = 10 deg).

B. Assessing the Chebyshev Criterion

The example presented in the preceding section focused on a Bolza problem. In other words, the weight factors K_1 and K_2 in the composite performance index (24) were set to zero. In the two numerical examples presented in this section, a zero value for the factor K_2 is maintained and K_1 is parametrically varied. A power, $n = 6$, has been adopted in the integral term J_1 of the composite index in both examples.

The first example concerns evaluation of optimal lateral escape trajectories in the baseline scenario for an assumed aerodynamic roll angle limit of 10 deg. Figures 4a–4e present results pertaining to three different values of K_1, namely, $K_1 = 0, 0.025$, and 25. The case $K_1 = 0$ represents the original Bolza problem, whereas $K_1 = 25$ represents a virtually pure Chebyshev problem.

Figure 4a shows the ground tracks of the resulting optimal escape trajectories. Figures 4b and 4c present the time histories of the two control variables: angle-of-attack and aerodynamic roll angle. The third control variable is throttle setting. Obviously, full throttle is used throughout the escape maneuver. It can be seen that the angle-of-attack behaviors for $K_1 = 0$ and 0.025 are very similar. Nevertheless, the resulting altitude profiles are quite different, as shown in Fig. 4d. In particular, the minimum altitude achieved is significantly higher for the trajectory computed for $K_1 = 0.025$. Furthermore, we note that a massive further increase in the parameter K_1 by a factor of 1000 (from $K_1 = 0.025$ to 25) leads to only a modest improvement in the actually achieved minimum altitude. However, the angle-of-attack behavior is quite different for the latter case, especially in the initial phase of the encounter. Some striking features in the angle-of-attack behavior for the cases $K_1 = 0.025$ and 25 concern the discontinuities in $d\alpha/dt$. The instances where these "cusps" in the time histories occur actually represent the entry points to the altitude-constrained subarcs that are present in both trajectories. Note that, on these constrained subarcs, angle of attack is effectively governed by Eq. (26). The trajectory for $K_1 = 25$ also features an additional touch point to the altitude constraint in the aftershear region.

Similar to angle-of-attack α, the behavior of the aerodynamic roll angle μ is not significantly affected by a slight increase in K_1. Only when K_1 is increased so that the Chebyshev part in the performance index becomes dominant is the aerodynamic roll angle behavior affected. Indeed, for $K_1 = 25$ the aerodynamic roll angle leaves its limit much earlier. However, as the decay seems almost completed, the aerodynamic roll angle suddenly starts to increase again and subsequently behaves similarly to the trajectories computed for low values of K_1. Note that the instance where this strange roll angle behavior occurs happens to be the final touch point to the altitude constraint. In a true Chebyshev problem, the behavior of the controls becomes virtually irrelevant once this final touch point has been passed. It is conjectured that, because of the heavily weighted Chebyshev part in the composite performance index, the emphasis initially is on maximizing the minimum altitude, but that attention is shifted toward minimizing the integral part once the minimum altitude constraint is definitively departed.

Up to this point, we have more or less implicitly assumed that $K_1 = 25$ is sufficiently large to represent a Chebyshev solution. To check this assumption, we have computed optimal lateral escape trajectories for a range of values of K_1 rather than just the three aforementioned values. The results are summarized in Fig. 4e, which shows how the integral part J_1 and the Chebyshev part J_2 in the composite performance index vary with K_1 in the optimal solution. Note that a logarithmic scale is used for the parameter K_1 in Fig. 4e. As expected, the value of J_1 monotonically increases

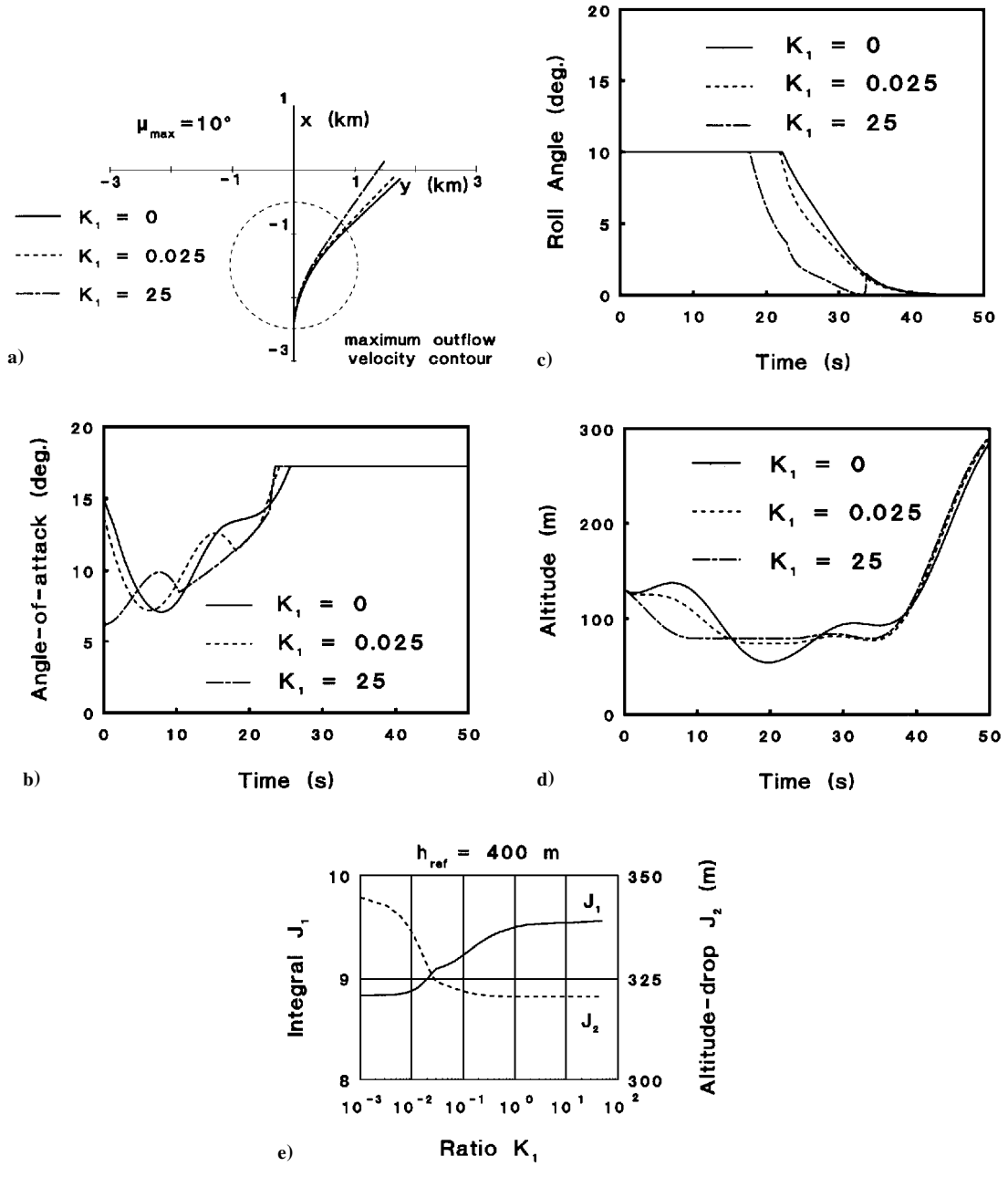

Fig. 4 Comparison of extremal solutions for various values of K_1. $K_2 = 0$; lateral maneuvering ($\mu_{max} = 10$ deg).

with K_1, whereas J_2 monotonically decreases with K_1. What really comes as a surprise is the magnitude in the variations of the two performance measures. By gradually moving from a Bolza problem to a Chebyshev problem, the minimum altitude performance can be improved by as much as 25 m. It seems safe to state that the Bolza approximation, as presently employed, is indeed rather poor. Another conclusion that can be drawn from Fig. 4e is that the absolute minimum altitude performance can be well approximated by solving the optimal control problem for any value of K_1 in excess of 0.1.

A striking feature that can be observed in the curves J_1 and J_2 vs K_1 in Fig. 4e is the slight cusp around $K_1 = 0.03$. The presence of this cusp can be explained from the fact that for values $K_1 > 0.03$, trajectories start featuring a touch point in addition to a constrained subarc. For values of $K_1 < 0.015$, the trajectories feature only a single touch point rather than a constrained subarc. In all, Fig. 4e thus comprises three different types of extremal trajectories, namely, trajectories featuring a single touch point, trajectories featuring a single constrained subarc, and trajectories featuring both a constrained subarc and a touch point.

A close examination of optimal Bolza solutions established in Ref. 5 revealed that the performance improvements offered by lateral escape maneuvers were a direct consequence of the fact that the passage through the shear region can be curtailed. These observations were fully reconfirmed in the present study. Whatever values are adopted for the weight factors K_1 and K_2, lateral maneuvering was always found to be beneficial relative to straight flight, at least for escapes that are initiated outside the peak outflow contour. Figure 5 demonstrates the benefits of lateral maneuvering by summarizing the results for a complete family of optimal trajectories, parameterized by K_1 and the imposed roll angle limit μ_{max}. Note that in a Chebyshev solution the extent of the constrained subarc decreases with an increasing roll angle limit. Indeed, when the roll angle limit is increased sufficiently, the constrained subarc reduces to a touch point.

In Ref. 14, additional numerical examples are presented, including several cases that involve forward-looking detection. The results obtained in Ref. 14 confirm the earlier observations that a lateral escape is especially effective in improving the recovery performance if advance warning is provided.[5]

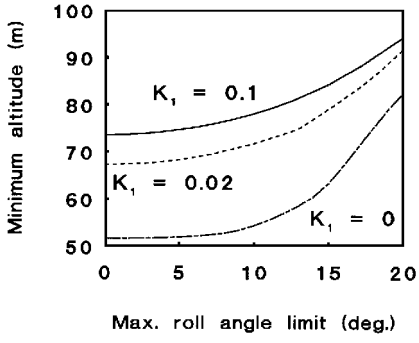

Fig. 5 Variation of minimum altitude with the specified value of the aerodynamic roll angle limit for various values of the weight factor K_1; $K_2 = 0$.

C. Assessing the Energy End-Cost

In the present study, lateral escape trajectories for nonzero values of K_2 in the performance index have been generated as well. Figure 6 presents the results for a typical example in which the following parameters have been adopted: $K_1 = 0.05$ and $\mu_{max} = 10$ deg. Four different values of K_2 are considered in Fig. 6.

A common feature of optimal solutions with a nonzero value for K_2 is that they all terminate with zero angle of attack. This particular feature is a direct consequence of the transversality conditions.[14] For relatively small values of K_2, the emphasis in the optimization process obviously still is on improving the minimum altitude performance. For increasing values of K_2, the emphasis shifts toward the maximum final energy criterion. This behavior is clearly demonstrated in Figs. 6a and 6b. For a small value of the factor K_2 (i.e., $K_2 = 0.005$) the angle-of-attack behavior within the shear region is virtually the same as that for the trajectory with $K_2 = 0$.

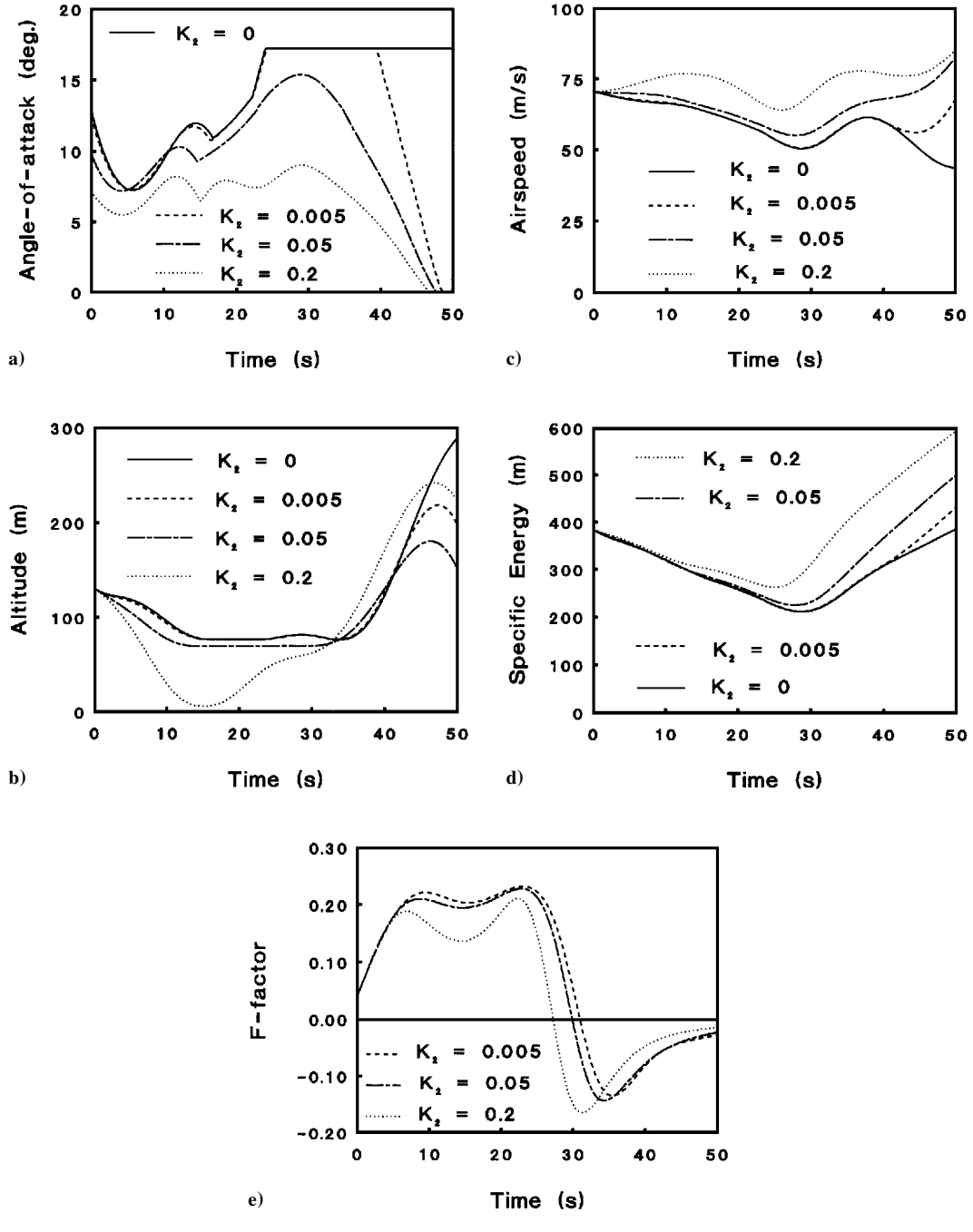

Fig. 6 Comparison of extremal solutions for various values of K_2. $K_1 = 0.05$; lateral maneuvering ($\mu_{max} = 10$ deg).

Consequently, the minimum altitude achieved also is almost the same for the two cases. Figure 6d shows that the effort to gain specific energy is confined to the aftershear region only. As the parameter K_2 is increased, the angle of attack will leave its limit earlier in the aftershear region. As a matter of fact, when K_2 is increased sufficiently, angle of attack will no longer reach its limit. This is evident in the solution for the value $K_2 = 0.05$ (the same value as used for K_1). In this particular case, the controls are noticeably influenced already within the shear region. Indeed, it is clear that minimum altitude is traded for an additional gain in specific energy. Figure 6b also reveals that the optimal trajectory no longer has a touch point in the aftershear region, i.e., only a constrained subarc is present.

For the value $K_2 = 0.2$, the minimum altitude is only 6 m. Clearly, the solution exhibits only a single touch point for this particular value of K_2. From a practical point of view, the resulting trajectory is hardly realistic; however, it does illustrate the tradeoff between maximizing minimum altitude and maximizing final specific energy. Figure 6e reveals that directing an aircraft to a low altitude leads to improved F-factor behavior. This can be largely attributed to the fact that an aircraft's exposure to downdraft is diminished at lower altitudes.

The specification of even a modest value of K_2 helps to avoid low airspeeds in the aftershear region (see Fig. 6c). Nevertheless, the overall behavior in the terminal phase is still far from desirable from an operational perspective. Indeed, in the final phase, trajectories with nonzero values for K_2 terminate with a dive. In Ref. 14 it is shown that this undesirable behavior can be simply avoided (without sacrificing performance) by specifying a nonnegative terminal value for flight path angle.

V. Concluding Remarks

Optimal lateral escape trajectories in a microburst wind field were studied for an aircraft on final approach. The performance index being minimized was the peak value of altitude drop, with the additional consideration of maximizing final specific energy. Minimizing the altitude drop can be achieved by directly solving the associated Chebyshev problem but also by approximating the minimax performance index by a Bolza integral. The latter approach is mathematically much simpler and therefore has generally been the method of choice up to this point. In this paper, a new composite performance index has been introduced, allowing a problem to be solved as a weighted combination of a Chebyshev term, an integral term, and a maximum final specific energy term.

Probably the most striking result obtained in this study relates to the dramatic improvement in minimum altitude performance that can be obtained by increasing the weight factor multiplying the Chebyshev term in the performance index. This leads us to believe that the previously used Bolza performance index approximation is not really all that useful. As a matter of fact, because this Bolza approximation is fairly widely used, this conclusion may have a much wider bearing than just the present windshear problem.

A close examination of the numerical results has revealed that the improvement in minimum altitude performance with increasing emphasis on the Chebyshev part is primarily realized by reducing angle of attack in the initial phase of the microburst encounter. Indeed, a Chebyshev solution appears to rapidly trade altitude for speed, such as to reduce the exposure to downdraft.

Inclusion of a relatively small final specific energy term in the performance criterion turned out to be useful in improving trajectory behavior in the aftershear region without affecting the minimum altitude performance. However, if the final specific energy term is heavily weighted, the overall trajectory behavior is influenced in the sense that altitude performance is sacrificed for the benefit of gaining specific energy.

A very important finding in the present study is that the benefits of lateral maneuvering vis-à-vis nonturning escape remain unchallenged. However, we must remain aware of the fact that in this study highly idealized (axisymmetric) windshear models have been used. In reality, spatial wind variations will generally exhibit far more erratic behavior than our simple model suggests. Another concern that has not yet been addressed relates to the occurrence of multiple simultaneous microbursts, possibly in different stages of development. A study on optimal escape trajectories in a complex wind flowfield is clearly warranted, obviously with due consideration to the probability of occurrence of such events.

References

[1]Visser, H. G., "Optimal Lateral Escape Maneuvers for Microburst Encounters During Final Approach," Delft Univ. of Technology, Rept. LR-691, Delft, The Netherlands, July 1992.

[2]Miele, A., Wang, T., and Melvin, W. W., "Optimization and Acceleration Guidance of Flight Trajectories in a Windshear," *Journal of Guidance, Control, and Dynamics*, Vol. 10, No. 4, 1987, pp. 368–377.

[3]Miele, A., Wang, T., and Melvin, W. W., "Penetration Landing Guidance Trajectories in the Presence of Windshear," *Journal of Guidance, Control, and Dynamics*, Vol. 12, No. 6, 1989, pp. 806–814.

[4]Miele, A., Wang, T., Melvin, W. W., and Bowles, R. L., "Acceleration, Gamma and Theta Guidance for Abort Landing in a Windshear," *Journal of Guidance, Control, and Dynamics*, Vol. 12, No. 6, 1989, pp. 815–821.

[5]Visser, H. G., "Optimal Lateral-Escape Maneuvers for Microburst Encounters During Final Approach," *Journal of Guidance, Control, and Dynamics*, Vol. 17, No. 6, 1994, pp. 1234–1240.

[6]Miele, A., and Wang, T., "An Elementary Proof of a Functional Analysis Result Having Interest for Minimax Optimal Control of Aeroassisted Orbital Transfer Vehicles," Rice Univ., Aero-Astronautics Rept. 182, Houston, TX, 1985.

[7]Bulirsch, R., Montrone, F., and Pesch, H. J., "Abort Landing in the Presence of Windshear as a Minimax Optimal Control Problem, Part 1: Necessary Conditions," *Journal of Optimization Theory and Applications*, Vol. 70, July, 1991, pp. 1–23.

[8]Bulirsch, R., Montrone, F., and Pesch, H. J., "Abort Landing in the Presence of Windshear as a Minimax Optimal Control Problem, Part 2: Multiple Shooting and Homotopy," *Journal of Optimization Theory and Applications*, Vol. 70, Aug. 1991, pp. 223–254.

[9]Oberle, H. J., "Numerical Treatment of Minimax Optimal Control Problems with Application to the Reentry Flight Path Problem," *Journal of the Astronautical Sciences*, Vol. 36, Nos. 1/2, 1988, pp. 159–178.

[10]Warga, J., "Minimizing Variational Curves Restricted to a Preassigned Set," *Transactions on the American Mathematical Society*, Vol. 112, 1964, pp. 432–455.

[11]Zhao, Y., and Bryson, A. E., "Optimal Paths Through Downbursts," *Journal of Guidance, Control, and Dynamics*, Vol. 13, No. 5, 1990, pp. 813–818.

[12]Visser, H. G., "Lateral Escape Guidance Strategies for Microburst Windshear Encounters," Delft Univ. of Technology, Memorandum M-723, Delft, The Netherlands, Feb. 1996.

[13]de Bruin, P. J., "Improved Models for Optimal Abort Landing Maneuvers in the Presence of Windshear," M.S. Thesis, Faculty of Aerospace Engineering, Delft Univ. of Technology, Delft, The Netherlands, Aug. 1995.

[14]Visser, H. G., "A Minimax Optimal Control Analysis of Lateral Escape Maneuvers for Microburst Encounters," Delft Univ. of Technology, Memorandum M-713, Delft, The Netherlands, Nov. 1995.